Chem Rev Lett 2 (2019) 140-150

Research Article

Chemical Review and Letters
journal homepage: www.chemrevlett.com
ISSN (online): 2645-4947 (print) 2676-7279

Adsorption behavior of the Al- and Ga-doped $B_{12}N_{12}$ nanocages on CO_n (n=1, 2) and H_nX (n=2, 3 and X=O, N): A comparative study

Hwda Ghafur Rauf [a], Evan Abdulkareem Mahmood [a], Soma Majedi [a,*], Mitra Sofi [b]

[a] *College of Health Sciences, University of Human Development, Sulaimaniyah, Kurdistan region of Iraq*
[b] *Department of Chemistry, Payame Noor University, Tehran, Iran*

ARTICLE INFO

Article history:
Received: 20 October 2019
Received in revised form: 9 December 2019
Accepted: 23 December 2019
Available online: 15 January 2020

Keywords:
Carbon monoxide
Carbon dioxide
Water
Ammonia
Al- and Ga-doped $B_{12}N_{12}$
M06-2X
Density functional theory
DFT

ABSTRACT

In this work, density functional theory (DFT) calculations are performed at the M06-2X/6-31+G* level to the adsorption of CO_n (n=1, 2) and H_nX (n=2, 3 and X=O, N) molecules onto pristine, Al- and Ga-doped $B_{12}N_{12}$ nanocages. We study the effect of Al- and Ga-doped on the sensing properties of $B_{12}N_{12}$ nanocage. This study clarifies the electrical behavior which obtained from interaction between the $B_{12}N_{12}$, Al- and Ga-doped $B_{12}N_{12}$ nanocages and CO_n (n=1, 2) and H_nX (n=2, 3 and X=O, N). The more stable structures are obtained on the minimum energy and non-imaginary vibrational frequencies. The results indicate a strong interactions obtained for the $B_{12}N_{12}$-NH_3, $AlB_{11}N_{12}$-NH_3 and $GaB_{11}N_{12}$-NH_3 complexes with values of -1.54, -2.32 and -2.34 eV. Calculations clarify that the Al-doped $B_{12}N_{12}$ can significantly improve both the adsorption energy and electronic properties of nanocage to NH_3. Finally, the Al-doped $B_{12}N_{12}$ is awaited to be a potential novel sensor for indicating the presence CO_n (n=1, 2) and H_nX (n=2, 3 and X=O, N) molecules.

1. Introduction

Ammonia (NH_3) gas is used as a solvent in many industries like fertilizers, plastic, petrochemical, textiles, pesticides [1,2], also is known to be extremely harmful to the human body and also a main cause of air pollution.

Carbon monoxide (CO) is one of the outstanding pollutant gases in the circumference, mostly produced by automobiles and industrial process. About 5 ppm concentration of CO in atmosphere is dangerous for human health [3]. It is plays a significant role in solving environmental difficulties such refinement air and atmosphere filtration [4-8].

Carbon dioxide (CO_2) is a colorless and odorless gas vital to life on Earth. It is used in the carbonated beverage industry, production of carbonates, carbon monoxide, carboxylic acids, such as present in deposits of petroleum and natural gas [9]. Its concentration approximately 50000 ppm reasons respiratory difficulties along with a number of other indications.

Water (H_2O) is a liquid at standard ambient temperature and pressure, but it often co-exists on earth in its solid state, ice or gaseous state, steam (water vapor). It also exists as snow, fog, dew and cloud. Water is present as vapor in atmosphere of the Sun [10] and Earth's atmosphere [11] etc.

Nano structures have attracted to the chemist for special properties and interesting character and applications [12-15]. Boron nitride nanocages have remarkable chemical and physical properties particularly due to showing the semiconductor properties [16–20]. Because of the polar nature of B-N bonds, the $B_{12}N_{12}$ nanocage are anticipated to have more reactivity than the C_{24} cage. For example, theoretical probes displayed that the $B_{12}N_{12}$ nanocage could store H_2 molecules with

* Corresponding author. e-mail: soma.majedi@uhd.edu.iq

more ease than the C_{24} nanocage [21]. It has been indicated that the $B_{12}N_{12}$ nanocage could be nice candidate for hydrogen adsorption on the surface this cages. Thus, significant charge dissociation between the B and N atoms, the B atom (electron deficient) and N atom (electron rich) can be used as Lewis acid and base, respectively. Therefore, the $B_{12}N_{12}$ nanocluster can be considered as a nanometal catalyst with Lewis acid-base pairs. The $B_{12}N_{12}$ nanocage is the most stable structure between several types of $(BN)_n$ structures [22]. Theoretical investigates indicated that the $B_{12}N_{12}$ nanocage is the more stable between $B_{12}N_{12}$, $B_{16}N_{16}$, $B_{28}N_{28}$ nanocages [23]. The boron nitride nanocage contains from four– and six–membered rings [24–28]. Beheshtian et al. [29] suggested that the $B_{12}N_{12}$ cluster can be applied to storage CO with an exothermic process. Ahmadi et al. have presented the electronic properties of carbon monoxide on Al- and Ga-doped single-walled BN nanotubes [30]. They have stated that the adsorption of CO on the Al-BNNT is more qualified than that of the Ga-BNNT. Shakerzadeh et al. theoretical studied the phosgene adsorption onto pristine, Al- and Ga-doped $B_{12}N_{12}$ and $B_{16}N_{16}$ nanoclusters [31]. Therefore, the obtained results for both clusters are nearly the same, which imply to this fact that the adsorption process is independent of cluster size. Kalateh and co-workers [32] have offered the adsorption treatment of H_2S on the surface of $B_{12}N_{12}$ and $AlB_{11}N_{12}$ fullerene at the B3LYP/6-31G* level of density functional theory.

In this work, $B_{12}N_{12}$ and its Al- and Ga-doped derivatives were selected as absorbent for carbon monoxide (CO), carbon dioxide (CO_2), water (H_2O) and ammonia (NH_3). Geometry optimizations, interaction energy, NBO charge transfer and energy gap are calculated and results were reported.

2. Computational details

Full geometry optimization, density of states (DOS), molecular electrostatic potential (MEP) frontier molecular orbitals (FMO) analyses, and adsorption energy calculations were done at the M06-2X level with 6-31+G* basis set as implemented in Gaussian 09 suite of program [33]. All the calculations carried out in the gas phase under 1atm pressure and 298K temperature. The E_{ad} was obtained *via* between the total energies of the adsorbent-nanocages complexes and the energies of each monomer. The interaction energies were reformed for the basis set superposition error (BSSE) in all the systems using the full counterpoise method [34]. The vibration frequencies were also calculated at the same level to determine that all the

3. Results and Discussion

3.1. Optimized the $B_{12}N_{12}$ and Al- and Ga-doped $B_{12}N_{12}$ nanocages

The optimized structures of the pristine and Al- and Ga-doped $B_{12}N_{12}$ nanocages at the M06-2X/6-31+G* level are shown in Fig. 1. The B–N, Al–N and Ga–N bond length between two hexagonal rings are 1.439, 1.432 and 1.431 Å and that is between a four- and a six-membered ring are 1.48, 1.82 and 1.89 Å. The energy difference between the highest occupied molecular orbital (HOMO) and the lowest un-occupied molecular orbital (LUMO), E_g of pristine and Al- and Ga-doped $B_{12}N_{12}$ nanocages are calculated to be 9.15, 6.58 and 6.14 eV, respectively. The highest occupied molecular orbital (HOMO) are localized on the nitrogen atom and the lowest un-occupied molecular orbital (LUMO) of the pristine and Al- and Ga-doped $B_{12}N_{12}$ nanocages are localized on the boron, aluminum and gallium atoms, respectively. The boron, aluminum and gallium atoms of nanocages acts as an electron acceptor (Lewis acid) and the nitrogen atoms of nanocages acts as an electron donor (Lewis base).

3.2. Adsorption of NH_3, CO, CO_2 and H_2O on the $B_{12}N_{12}$ and Al- and Ga-doped $B_{12}N_{12}$ nanocages

Air pollutant and toxic molecules including NH_3, CO, CO_2 and H_2O were chosen as the adsorbents. We performed full structural optimization on monomers and complexes to investigate the energetic, equilibrium geometries and electronic properties. The values of adsorption energy (E_{ads}), adsorbent-nanocages interaction distance ($d_{(adsorbent\text{-}nanocages)}$), natural bonding orbital (NBO) analysis and the ΔE_g (change of E_g of cage upon the adsorption process) are presented in Table 1.

3.2.1. Adsorption of NH_3 on the nanocages

Fig. 1 shows optimized structures and complexes at the M06-2X/6-31+G* level of calculations. After the geometry optimization, stable systems were observed for adsorption processes NH_3─$B_{12}N_{12}$, NH_3─$AlB_{11}N_{12}$ and NH_3─$GaB_{11}N_{12}$ complexes. The adsorption energies (E_{ads}) for NH_3─$B_{12}N_{12}$, NH_3─$AlB_{11}N_{12}$ and NH_3─$GaB_{11}N_{12}$ complexes are -1.54, -2.32 and -2.34 eV, and values of adsorbent-nanocages distances are 1.62, 1.98 and 2.04 Å, respectively. The charge transfers from nitrogen of NH_3 to the boron, aluminum and gallium atoms of nanocages are 0.56, 0.17 and 0.18 e, respectively, showing high polarity nature of these bonds. Calculated molecular electrostatic potential

displays that the nitrogen atom of NH_3 acts as an electron donor Lewis base and the boron atom of cage acts as an electron acceptor. The FMO analysis on the NH_3 sensor, showing that its energy gaps for NH_3─$B_{12}N_{12}$, NH_3─$AlB_{11}N_{12}$ and NH_3─$GaB_{11}N_{12}$ complexes are about 7.72, 6.91 and 6.87 eV, respectively.

3.2.2. Adsorption of CO on the nanocages

Three complexes were found in order to study the adsorption of CO on the pristine and Al- and Ga-doped $B_{12}N_{12}$ nanocages. The C─side and O─side of CO adsorb on the top of the boron, aluminum and gallium atoms of nanocages (Fig. 1). The calculations show that the CO─$B_{12}N_{12}$, CO─$AlB_{11}N_{12}$ and CO─$GaB_{11}N_{12}$ systems are exothermic processes with negative adsorption energies.

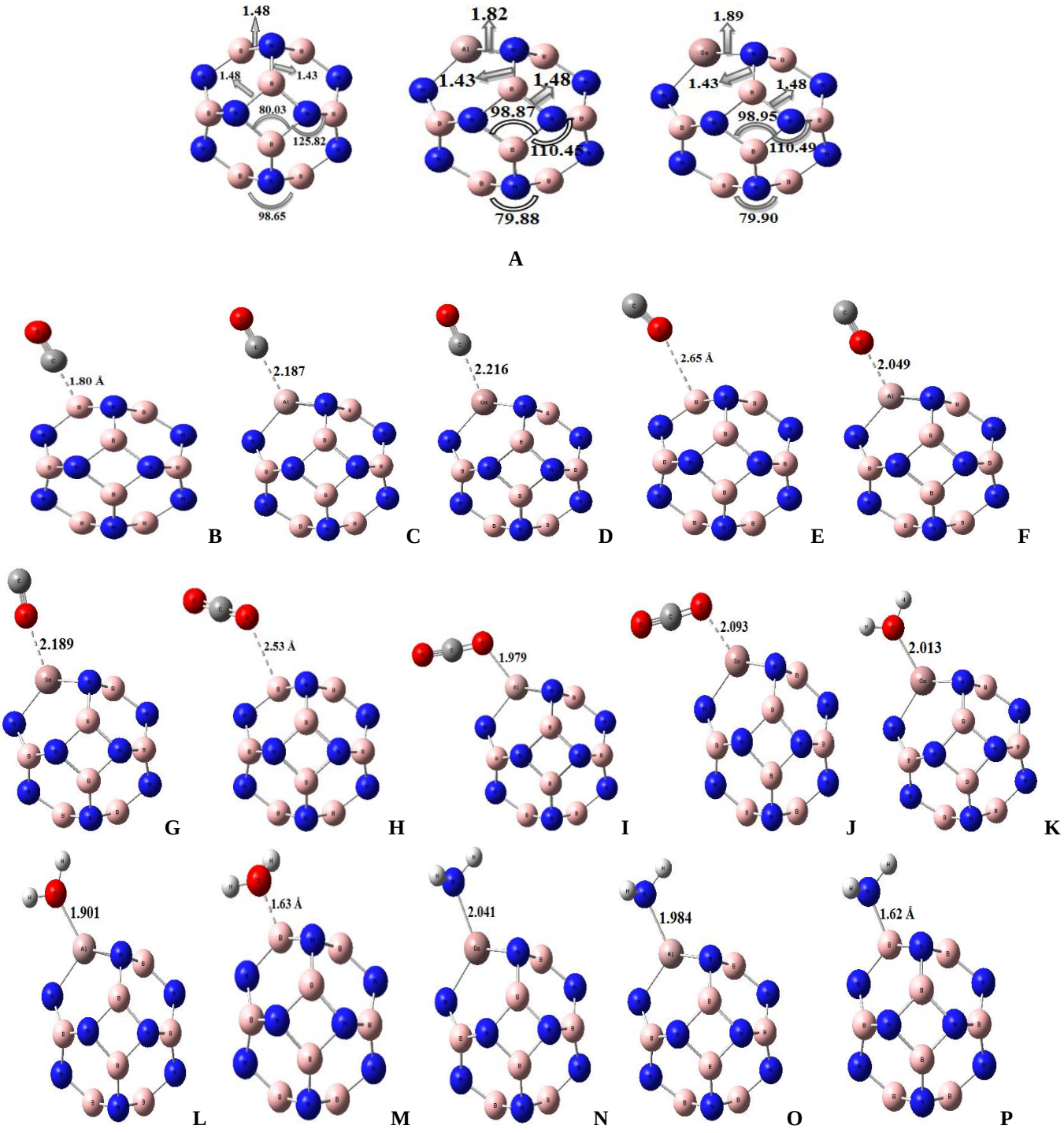

Fig. 1. Geometric parameters of pure $B_{12}N_{12}$, Al- and Ga-doped $B_{12}N_{12}$ and absorbents/nanocages. Distances in Å and angles in degree

Table 1. Calculated equilibrium adsorbent-nanocages distance ($d_{adsorbate-nanocages}$), adsorption energy (E_{ad}: eV), HOMO energies (E_{HOMO}), LUMO energies (E_{LUMO}) and HOMO–LUMO energy gap (E_g) for mentioned Configurations.

Configurations	$d_{Molecule/B_{12}N_{12}}$	E_{ad}	Q_{NBO}	E_{HOMO} (eV)	E_{LUMO} (eV)	E_g (eV)	$^a\Delta E_g$ (%) (eV)
$B_{12}N_{12}$	─	─	─	-9.51	-0.36	9.15	─
$B_{12}N_{12}$-NH_3	1.62	-1.54	0.56	-8.68	-0.95	7.72	142.59
$B_{12}N_{12}$-H_2O	1.64	-0.87	0.29	-8.86	-0.99	7.88	127.05
$B_{12}N_{12}$-CO_2	2.54	-0.14	0.04	-9.44	-0.44	9.00	14.69
$B_{12}N_{12}$-CO(C─side)	1.81	-0.15	1.20	-9.14	-0.05	9.09	5.87
$B_{12}N_{12}$-CO(O─side)	2.66	-0.09	0.02	-9.45	-0.01	9.44	29.01
$AlB_{11}N_{12}$	─	─	─	-9.08	-2.51	6.58	─
$AlB_{11}N_{12}$-NH_3	1.98	-2.32	0.17	-8.36	-1.46	6.91	32.93
$AlB_{11}N_{12}$-H_2O	1.90	-1.83	0.14	-8.44	-1.75	6.68	10.64
$AlB_{11}N_{12}$-CO_2	1.98	-0.87	0.12	-8.71	-1.28	7.43	85.17
$AlB_{11}N_{12}$-CO(C─side)	2.19	-0.85	0.25	-8.75	-2.68	6.07	50.42
$AlB_{11}N_{12}$-CO(O─side)	2.05	-0.54	0.10	-8.76	-2.29	6.47	10.83
$GaB_{11}N_{12}$	─	─	─	-9.06	-2.92	6.14	─
$GaB_{11}N_{12}$-NH_3	2.04	-2.34	0.18	-8.30	-1.42	6.87	72.85
$GaB_{11}N_{12}$-H_2O	2.01	-1.67	0.13	-8.39	-1.65	6.74	59.73
$GaB_{11}N_{12}$-CO_2	2.09	-0.83	0.11	-8.71	-1.42	7.28	114.05
$GaB_{11}N_{12}$-CO(C─side)	2.22	-0.99	0.26	-8.68	-2.57	6.11	3.78
$GaB_{11}N_{12}$-CO(O─side)	2.19	-0.59	0.09	-8.75	-1.83	6.93	78.94

[a]The change of HOMO–LUMO gap of $B_{12}N_{12}N$ after adsorption. All energies are in eV. All distances are in Å. Q_{NBO} is in e.

For C─side interaction, E_{ad} (adsorbent-nanocages interaction distance) are -0.15 (1.81 Å), -0.85 (2.19 Å), respectively. For O─side interaction, E_{ad} (adsorbent-nanocages interaction distance) are -0.99 (2.22 Å) eV and -0.09 (2.66 Å), -0.54 (2.05 Å) and -0.59 (2.19 Å) eV respectively, (Fig. 1 and Table 1). Therefore, we can conclude that the C─side interaction is stronger than that of O─side interaction. The DFT calculations showed the charge transfers of 1.20, 0.25 and 0.26 e from C─side of CO to the B, Al and Ga atoms of nanostructures and 0.02, 0.10 and 0.09 e from O─side of CO to the boron, aluminum and gallium atoms of cages. The calculated MEP displays electron rich regions with red and electron deficient regions with blue color (Fig. 2).

The FMO analysis shows that the interactions between the C─side and O─side of CO and B, Al and Ga atoms of the pristine and Al- and Ga-doped $B_{12}N_{12}$ nanocages were carried out which HOMO locates at the C as well as O atoms and LUMO locates at the B, Al and Ga of the nanocages, respectively (Fig. 3).

3.2.3. Adsorption of CO_2 on nanocages virtues

The optimized structures for the most stable configurations CO_2─$B_{12}N_{12}$, CO_2─$AlB_{11}N_{12}$ and CO_2─$GaB_{11}N_{12}$ complexes are presented in Fig. 1. The adsorption energies are -0.14, -0.87 and -0.83 eV and the adsorbent-nanocages distance are 2.54, 1.98 and 2.09 Å, respectively. The charges of 0.040, 0.125 and 0.115 e are transferred from CO_2 to the boron, aluminum and gallium atoms of nanocages (Table 1). Electrostatic potential analysis which displays at the 0.001 electrons per $Bohr^{-3}$ isodensity surfaces were calculated with WFA surface analysis (Fig. 2) [35].

DFT calculations shows the electron transfer from the HOMO of CO_2 to the LUMO on the boron, aluminum and gallium atom of the cages (Fig. 3). The HOMO–LUMO energy gap (E_g) for the CO_2─$B_{12}N_{12}$, CO_2─$AlB_{11}N_{12}$ and CO_2─$GaB_{11}N_{12}$ systems are 9.00, 7.43 and 7.28 eV, respectively (Table 1)

3.2.4. Adsorption of H_2O on nanocages virtues

We investigate the adsorption of H_2O on the pristine and Al- and Ga-doped $B_{12}N_{12}$ nanocages (Fig. 1). The adsorbent-nanocages distance for H_2O─$B_{12}N_{12}$, H_2O─$AlB_{11}N_{12}$ and H_2O─$GaB_{11}N_{12}$ are 1.64, 1.90 and 2.01 Å and the adsorption energies (E_{ad}) are -0.87, -1.83 and -1.67 eV, respectively. The NBO calculations reveal that the charge transfers from oxygen of H_2O to boron, aluminum and gallium atoms of cages are 0.29, 0.140 and 0.134 e, respectively (Table 1).

Therefore, boron, aluminum and gallium atoms of

cages act as Lewis acid site and the oxygen atom of water acts as Lewis base site.

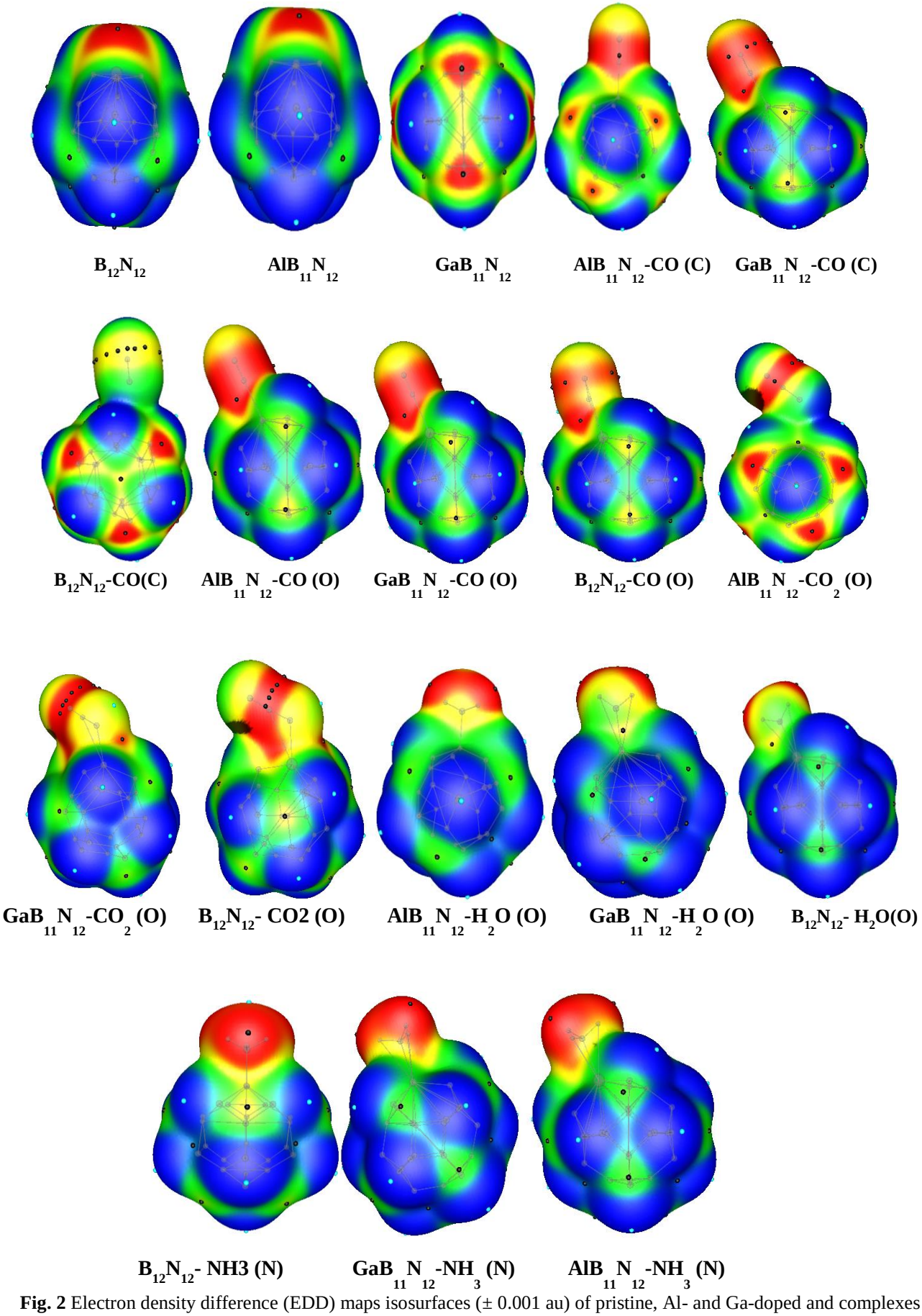

Fig. 2 Electron density difference (EDD) maps isosurfaces (± 0.001 au) of pristine, Al- and Ga-doped and complexes

Name	HOMO	LUMO
$B_{12}N_{12}$	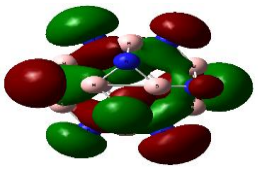	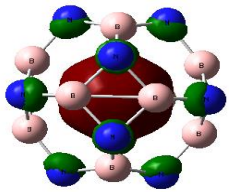
$AlB_{11}N_{12}$	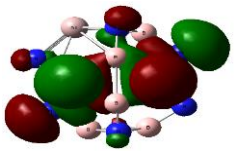	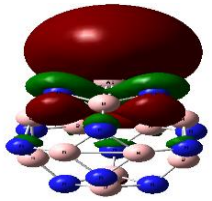
$GaB_{11}N_{12}$	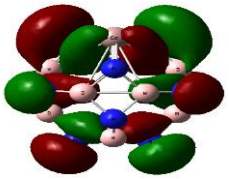	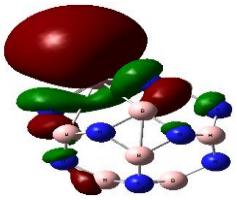
$B_{12}N_{12}$-CO(C)	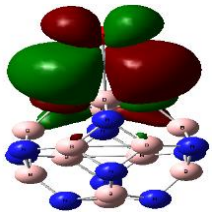	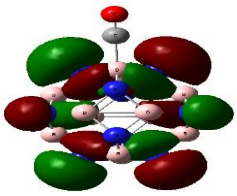
$AlB_{11}N_{12}$-CO(C)	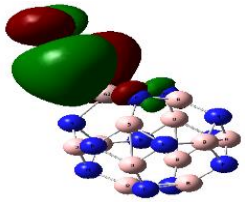	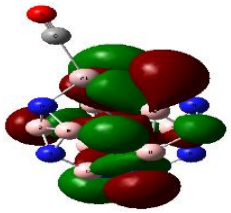
$GaB_{11}N_{12}$-CO(C)	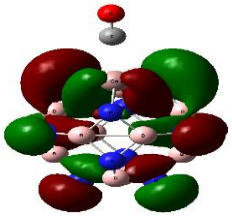	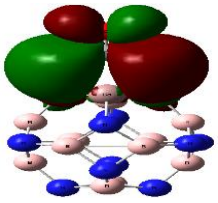
$B_{12}N_{12}$-CO(O)	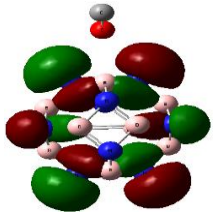	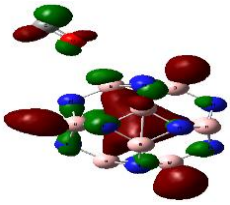
$AlB_{11}N_{12}$-CO(O)	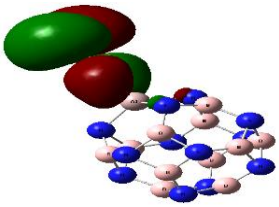	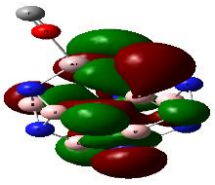

Name	HOMO	LUMO
$GaB_{11}N_{12}$-CO(O)	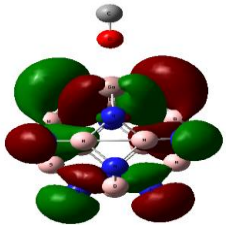	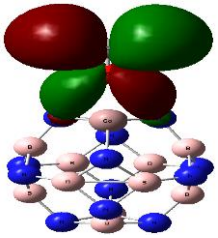
$B_{12}N_{12}$-CO2(O)	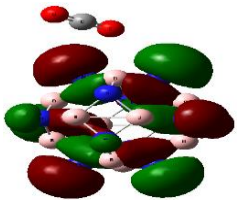	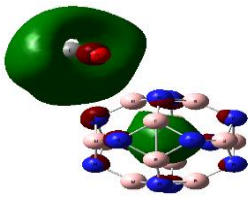
$AlB_{11}N_{12}$-CO_2(O)	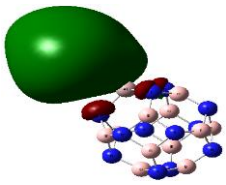	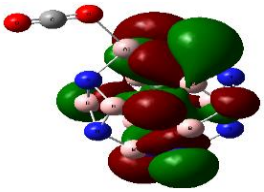
$GaB_{11}N_{12}$-CO_2(O)	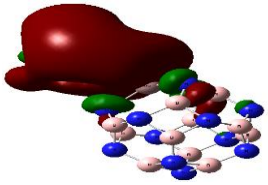	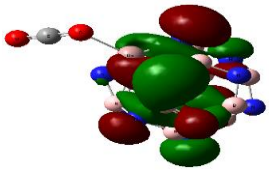
$B_{12}N_{12}$-H_2O(O)	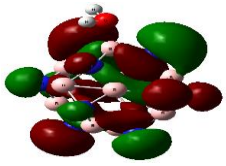	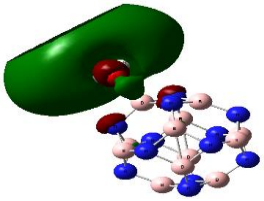
$AlB_{11}N_{12}$-H_2O(O)	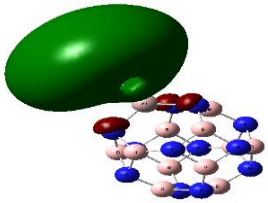	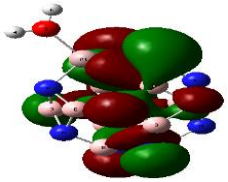
$GaB_{11}N_{12}$-H_2O(O)	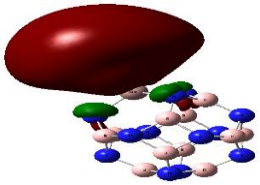	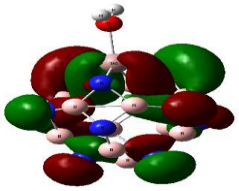
$B_{12}N_{12}$-NH_3(N)	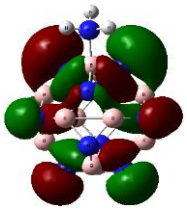	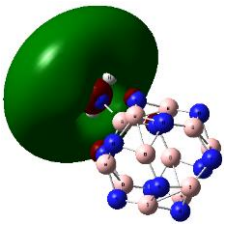

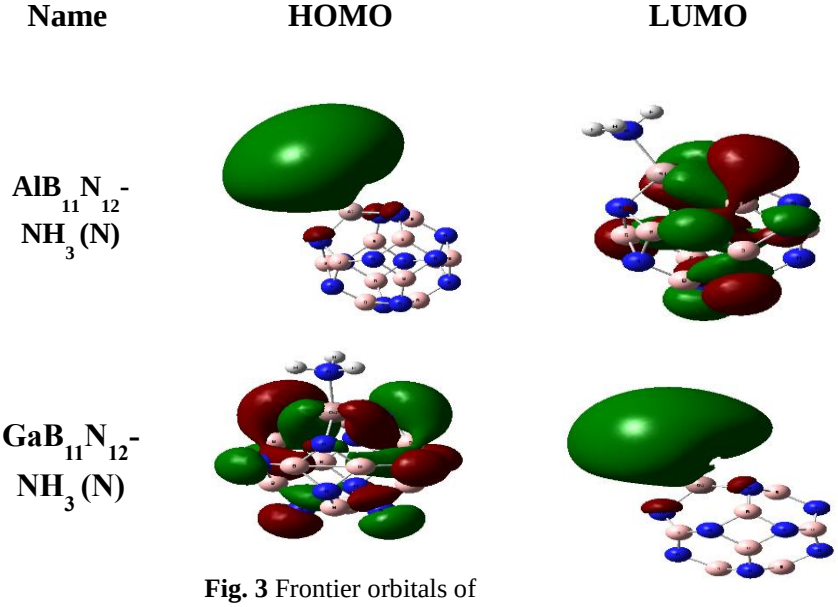

Fig. 3 Frontier orbitals of mentioned Configurations

The most positive and most negative potentials that defined as $V_{S,max}$ and $V_{S,min}$, respectively are shown in Fig. 2 (Table 1). The HOMO–LUMO gap (E_g) for the H_2O─$B_{12}N_{12}$, H_2O─$AlB_{11}N_{12}$ and H_2O─$GaB_{11}N_{12}$ systems are 7.88, 6.68 and 6.74 eV, respectively (Fig. 3).

Adsorption energy difference in the mentioned complexes attributed to the basis of electronegativity difference, p character, and dipole moment in the molecules (Table 2).

3.3. Density of state analysis

To investigate the adsorption effects of the CO_n (n=1, 2) and H_nX (n=2, 3 and X=O, N) molecules over the $B_{12}N_{12}$, $AlB_{11}N_{12}$ and $GaB_{11}N_{12}$, the density of states DOS for the most stable systems of the adsorbent/nanocages complexes was studied which shown in Fig. 4. In mentioned complexes, the DOS near the Fermi level are not affected upon the adsorptions process and E_g of the cages has no significant change at the M06-2X/6-31+G* level of theory (Table 1). The change of HOMO–LUMO gap ($\%\Delta E_g$) in the adsorption process is associated to the sensitivity of an absorbent for a particular molecule. As seen in Table 1, the ΔE_g for NH_3─$B_{12}N_{12}$, NH_3─$AlB_{11}N_{12}$ and NH_3─$GaB_{11}N_{12}$, CO(C─side)─$B_{12}N_{12}$, CO(C─side)─$AlB_{11}N_{12}$ and CO(C─side)─$GaB_{11}N_{12}$, CO(O─side)─$B_{12}N_{12}$, CO(O─side)─$AlB_{11}N_{12}$ and CO(O─side)─$GaB_{11}N_{12}$ CO_2─$B_{12}N_{12}$, CO_2─$AlB_{11}N_{12}$ and CO_2─$GaB_{11}N_{12}$, H_2O─$B_{12}N_{12}$, H_2O─$AlB_{11}N_{12}$ and H_2O─$GaB_{11}N_{12}$ systems are 142.59%, 32.93%, 72.85%, 5.87%, 50.42%, 3.78%, 29.01%, 10.83%, 78.94%, 14.69%, 85.17%, 114.05%, 127.05%, 10.64% and 59.73%, respectively. It is known that the E_g is a major factor in determination of the electrical conductivity of $B_{12}N_{12}$, $AlB_{11}N_{12}$ and $GaB_{11}N_{12}$ which will improve in the existence of the molecules with respect to the following equation:

$$\sigma \propto \exp\left(\frac{-E_g}{2KT}\right)$$

Where σ is the electrical conductivity and k is the Boltzmann's constant. According to the equation, the smaller E_g amount leads to increase the conductivity at a given temperature. However, it can be conclude that the $B_{12}N_{12}$, $AlB_{11}N_{12}$ and $GaB_{11}N_{12}$ nanocages selectively act as a gas sensor device to the CO_2, CO, H_2O and NH_3 molecules which cages acts as the most appropriate gas sensor for the NH_3 molecule.

4. Conclusions

DFT calculations were carried out to study the equilibrium geometries, stabilities, and electronic properties of CO_n (n=1, 2) and H_nX (n=2, 3 and X=O, N) molecules which adsorbed at top of the $B_{12}N_{12}$, $AlB_{11}N_{12}$ and $GaB_{11}N_{12}$ nanocages. The results reveal that the CO_2, CO, NH_3 and H_2O molecules can be strongly adsorbed over the $B_{12}N_{12}$, $AlB_{11}N_{12}$ and $GaB_{11}N_{12}$ nanocages with a good adsorption energy.

Charge transfer from nitrogen, carbon or oxygen, oxygen, oxygen atoms of NH_3, CO, CO_2, and H_2O, respectively, to boron, aluminum and gallium atoms of

nanocages. Strong interaction between the electron deficient part of the nanocages and electron donating part of NH_3, CO, CO_2 and H_2O molecules observed. The most stable configurations were NH_3─$B_{12}N_{12}$ NH_3─$AlB_{11}N_{12}$ and NH_3─$GaB_{11}N_{12}$ with E_{ad} about –1.54, -2.32 and -2.34 eV, respectively. Finally, it is concluded that the $B_{12}N_{12}$, $AlB_{11}N_{12}$ and $GaB_{11}N_{12}$ nanocages has greater respond selectivity toward NH_3 compared to CO_2, CO and H_2O and it is consistent with the theoretical and experimental observation

Table 2. HOMO energies (E_{HOMO}), LUMO energies (E_{LUMO}) and HOMO–LUMO energy gap (E_g), dipole moment (D) and electronegativity of NH_3, H_2O, CO_2 and CO

analyte	E_{HOMO} (eV)	E_{LUMO} (eV)	E_g (eV)	dipole moment (D)	Electronegativity
NH_3	-9.06	1.42	10.48	1.86	-3.82
H_2O	-10.77	1.92	12.69	2.27	4.42-
CO_2	-12.28	-0.05	12.23	0.00	-6.16
CO	-12.25	0.26	12.50	0.01	-6.00

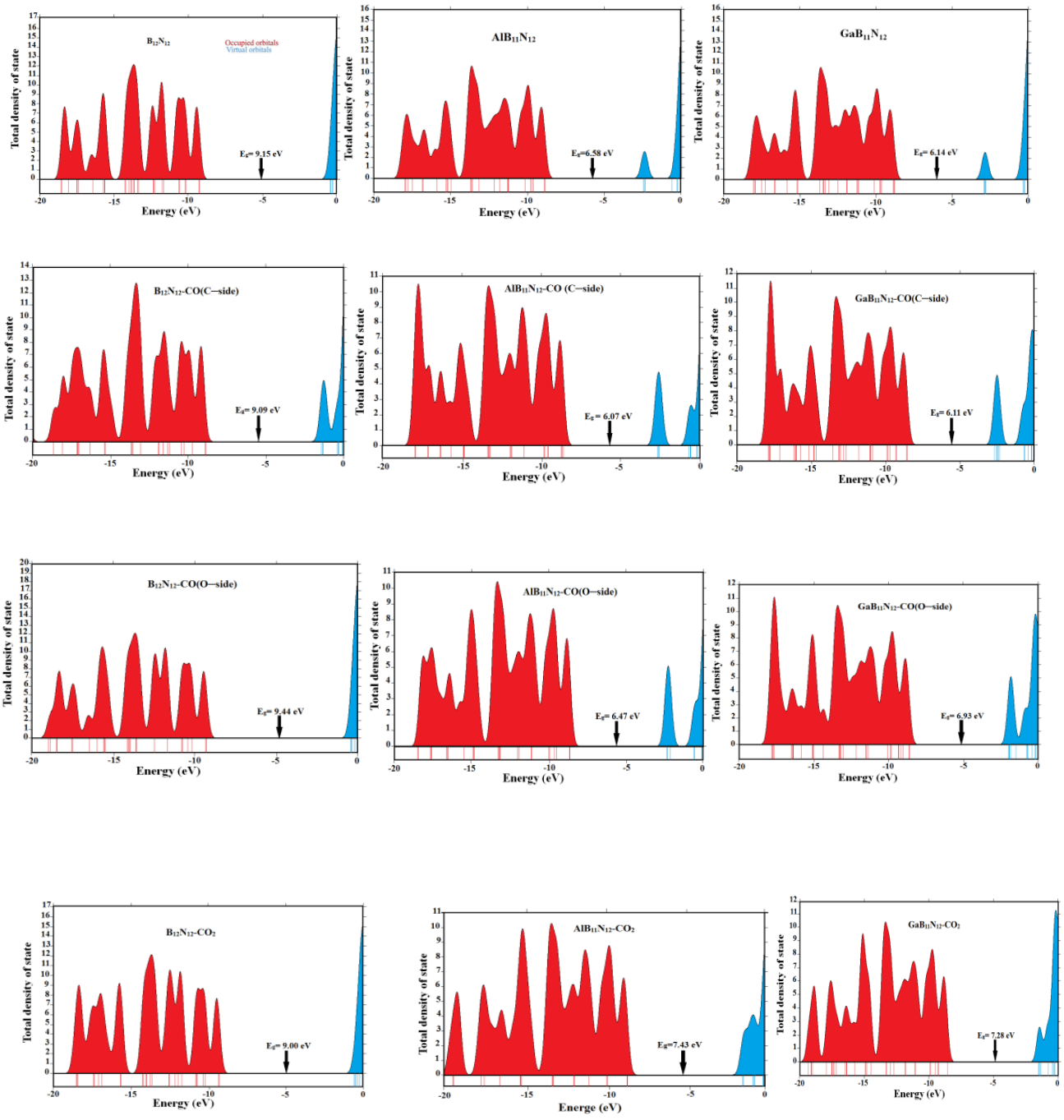

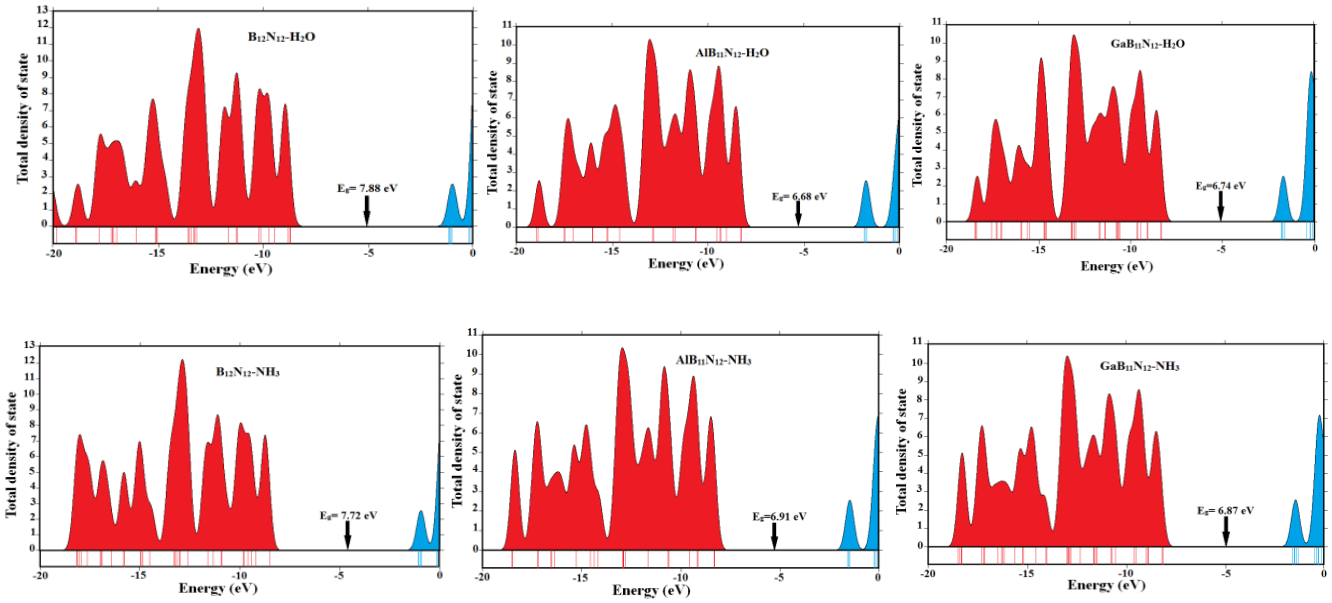

Fig. 4. Computed density of states (DOS) for monomers and complexes**.**

References

[1] S.Mahajan, Pollution control in process industries; Tata McGraw-Hill Education: Noida, India, (1985).

[2] B. Timmer, W. Olthuis, A. Berg, Ammonia sensors and their applications—a review, *Sensor Actuat B-Chem.* 107 (2005) 666-677.

[3] S. Sepaniak, T. Forges, H. Gerard, B. Foliguet, M. C. Bene, P. Monnier-Barbarino, The influence of cigarette smoking on human sperm quality and DNA fragmentation, *Toxicology*, 223 (2006) 54-60.

[4] H. J. Freund, G. Meijer, M. Scheffler, R. Schlçgl, M. Wolf, CO Oxidation as a Prototypical Reaction for Heterogeneous Processes, *Angew. Chem. Int. Ed.* 2011, 50, 10064–10094; *Angew. Chem.*, 123 (2011) 10242–10275.

[5] X. W. Xie, Y. Li, Z. Q. Liu, M. Haruta, W. J. Shen, Low-temperature oxidation of CO catalysed by Co(3)O(4) nanorods, *Nature*, 458 (2009) 746–749.

[6] S. Royer, D. Duprez, Catalytic Oxidation of Carbon Monoxide over Transition Metal Oxides, *Chem. Cat. Chem.* 3 (2011) 24–65.

[7] R. Kou, Y. Y. Shao, D. H. Mei, Z. Nie, D. H. Wang, C. M. Wang, V. V. Viswanathan, S. Park, I. A. Aksay, Y. H. Lin, Y. Wang, J. Liu, Stabilization of Electrocatalytic Metal Nanoparticles at Metal-Metal Oxide-Graphene Triple Junction Points, *J. Am. Chem. Soc*. 133 (2011) 2541–2547.

[8] E. J. Peterson, A. T. DeLaRiva, S. Lin, R. S. Johnson, H. Guo, J. T. Miller, J. Hun Kwak, C. H. F. Peden, B. Kiefer, L. F. Allard, F. H. Ribeiro, A. K. Datye, Low-temperature carbon monoxide oxidation catalysed by regenerable atomically dispersed palladium on alumina, *Nat. Commun*. 5 (2014) 1-11.

[9] I. C. Prentice, et al., The Carbon Cycle and Atmospheric Carbon Dioxide. In: Climate Change (2001).

[10] S. K. Solanki, W. Livingston, T. Ayres, New Light on the Heart of Darkness the Solar chromosphere, *Science*. 263 (1994) 64_66.

[11] R. Sridharan, S. M. Ahmed, T. P. Das, P. Sreelatha, P. Pradeepkumar, N. Naika, G. Supriya, Direct evidence for water (H2O) in the sunlit lunar ambience from CHACE on MIP of Chandrayaan I, *Planet. Space Sci*. 58 (2010) 947-950.

[12] I. Torkpoor, M. Heidari Nezhad Janjanpour, N. Salehi, F. Gharibzadeh, L. Edjlali, Insight into Y@X_2B_8 (Y= Li, CO_2 and Li-CO_2, X = Be, B and C) nanostructures: A computational study, Chem. Rev. Lett. 1 (2018) 2-8.

[13] R. Rostamoghli, M. Vakili, A. Banaei, E. Pourbashir, K. Jalalierad, Applying the $B_{12}N_{12}$ nanoparticle as a sensor for CO, CO_2, H_2O and NH_3 gasses, Chem. Rev. Lett. 1 (2018) 31-36.

[14] M. Heidari Nezhad Janjanpour, M. Vakili, S. Daneshmehr, K. Jalalierad, F. Alipour, Study of the Ionization Potential, Electron Affinity and HOMO-LUMO Gaps in the Small Fullerene Nanostructures, Chem. Rev. Lett. 1 (2018) 45-49.

[15] Siadati SA, Kula K, Babanezhad E, The possibility of a two-step oxidation of the surface of C20 fullerene by a single molecule of nitric (V) acid, Chem Rev Lett, 2019;2:2-6

[16] R.T. Paine, C.K. Narula, Synthetic routes to boron nitride, *Chem. Rev*. 90 (1990) 73-91.

[17] H.S. Wu, F.Q. Zhang, X.H. Xu, C.J. Zhang, H. Jiao, Geometric and Energetic Aspects of Aluminum Nitride Cages, *J. Phys. Chem. A* 107 (2003) 204-209.

[18] H.Y. Zhu, T.G. Schmalz, D.J. Klein, Alternant boron nitride cages: A theoretical study, *Int. J. Quantum Chem*. 63 (1997) 393-401.

[19] D. Goldberg, Y. Bando, O. Stepahan, K. Kurashima, Octahedral boron nitride fullerenes formed by electron beam irradiation, *Appl. Phys. Lett*. 73 (1998) 2441-2443.

[20] Q. Wang, Q. Sun, P. Jena, Y. Kawazoe, Potential of AlN Nanostructures as Hydrogen Storage Materials, *ACS Nano* 3 (2009) 621-626.

[21] T. Oku, A. Nishiwaki, I. Narita, M. Gonda, Formation and structure of $B_{24}N_{24}$ clusters, *Chem. Phys. Lett*. 380 (2003) 620-623.

[22] S. Xu, M. Zhang, Y. Zhao, B. Chen, J. Zhang, C.C. Sun, Stability and property of planar $(BN)_x$ clusters, *Chem. Phys. Lett*. 423 (2006) 212-214.

[23] G. Seifert, R. Fowler, D. Mitchell, D. Porezag, T. Frauenheim, Boron-nitrogen analogues of the fullerenes: electronic and structural properties, *Chem. Phys. Lett*. 268 (1997) 352-358.

[24] D. Strout, Structure and Stability of Boron Nitrides: Isomers of $B_{12}N_{12}$, *J. Phys. Chem*. A 104 (2000) 3364-3366.

[25] D. Strout, Structure and Stability of Boron Nitrides: The Crossover between Rings and Cages, *J. Phys. Chem. A* 105 (2001) 261-263.
[26] F. Jensen, H. Toftlund, Structure and stability of C_{24} and $B_{12}N_{12}$ isomers, *Chem. Phys. Lett*. 201 (1993) 89-96.
[27] T. Oku, A. Nishiwaki, I. Narita, Formation and atomic structure of B12N12 nanocage clusters studied by mass spectrometry and cluster calculation, *Sci. Technol. Adv. Mater*. 5 (2004) 635-638.
[28] T. Oku, M. Kuno, H. Kitahara, I. Nartia, Formation, atomic structures and properties of boron nitride and carbon nanocage fullerene materials, *Int. J. Inorg. Mater*. 3 (2001) 597-612.
[29] J. Beheshtian, Z. Bagheri, M. Kamfiroozi, A. Ahmadi, Toxic CO detection by $B_{12}N_{12}$ nanocluster, *Microelectron*. 42 (2011) 1400–1403
[30] A. Ahmadi Peyghan, A. Soltani, A. Allah Pahlevani, Y. Kanani, S. Khajeh, A first-principles study of the adsorption behavior of CO on Al- and Ga-doped single-walled BN nanotubes, *Applied Surface Science* 270 (2013) 25–32.
[31] E. Shakerzadeh, E. Khodayar, S. Noorizadeh, Theoretical assessment of phosgene adsorption behavior onto pristine, Al- and Ga-doped $B_{12}N_{12}$ and $B_{16}N_{16}$ nanoclusters, Comput. Mater. 118 (2016) 155–171.
[32] K. Kalateh, A. Abdolmanafi, Study of $B_{12}N_{12}$ and AlB11N12 fullerene as H2S absorbent and sensor by computational method, *Journal of New Chemistry*, 2 (2015) 172-178
[33] M. W. Schmidt, K. K. Baldridge, J. A. Boatz, S. T. Elbert, M. S. Gordon, J. H. Jensen, S. Koseki, N. Matsunaga, K. A. Nguyen, S. J. Su, T. L. Windus, M. Dupuis, J. A. Montgomery, General atomic and molecular electronic structure system, *J Comput. Chem*. 14 (1993)1347–1363.
[34] S. Iijima, C. J. Brabec, A.Maiti, J. Bernholc, Structural flexibility of carbon nanotubes, *J. Chem. Phys*. 104 (1996) 2089-2092.
[35] F. A. Bulat, A. Toro-Labbe, T. Brinck, J.S. Murray, P. Politzer, Quantitative analysis of molecular surfaces: areas, volumes, electrostatic potentials and average local ionization energies, *J. Mol. Model*. 16 (2010)1679 – 1691.

How to Cite This Article

Hwda Ghafur Rauf; Soma Majedi; Evan Abdulkareem Mahmood; Mitra Sofi. "Adsorption behavior of the Al- and Ga-doped B12N12 nanocages on COn (n=1, 2) and HnX (n=2, 3 and X=O, N): A comparative study". Chemical Review and Letters, 2, 3, 2019, 140-150. doi: 10.22034/crl.2020.214660.1029